PHYSICAL REVIEW A **91**, 021802(R) (2015)

Accurate multipixel phase measurement with classical-light interferometry

Mandeep Singh and Kedar Khare*
Department of Physics, Indian Institute of Technology, Delhi 110016, India

Anand Kumar Jha
Department of Physics, Indian Institute of Technology, Kanpur 208016, India

Shashi Prabhakar and R. P. Singh
Physical Research Laboratory, Ahmedabad 380009, India
(Received 7 September 2014; published 12 February 2015)

We demonstrate accurate phase measurement from experimental low photon level interferograms using a constrained optimization method that takes into account the expected redundancy in the unknown phase function. This approach is shown to have significant noise advantage over traditional methods, such as balanced homodyning or phase shifting, that treat individual pixels in the interference data as independent of each other. Our interference experiments comparing the optimization method with the traditional phase-shifting method show that when the same photon resources are used, the optimization method provides phase recoveries with tighter error bars. In particular, rms phase error performance of the optimization method for low photon number data (10 photons per pixel) shows a $>5\times$ noise gain over the phase-shifting method. In our experiments where a laser light source is used for illumination, the results imply phase measurement with an accuracy better than the conventional single-pixel-based shot-noise limit that assumes independent phases at individual pixels. The constrained optimization approach presented here is independent of the nature of the light source and may further enhance the accuracy of phase detection when a nonclassical-light source is used.

DOI: 10.1103/PhysRevA.91.021802 PACS number(s): 42.30.Rx, 42.25.Hz, 42.50.St

Interferometric phase detection is one of the most important techniques in physics. Optical interferometers are being used routinely for metrology, biomedical applications, Fourier transform spectroscopy, and holographic three-dimensional (3D) imaging, to name a few applications [1]. Sensitive phase detection is at the heart of large scale collaborative efforts such as gravitational wave detection [2]. Our aim in this Rapid Communication is to examine the interferometric phase-detection problem with an optimization framework that effectively models the redundancy in the unknown phase signal. For given photon resources, we show that this approach gives phase measurements with an accuracy better than the conventional single-pixel-based shot-noise limit (SNL) even when a classical-light source is used. This conclusion, though somewhat surprising, suggests that limits such as SNL may be generalized to incorporate the multipixel structure of the unknown phase signal. While the quantum limits to the measurement of stochastically fluctuating time-varying phases have been studied before, our focus in this work is to exploit the redundancy in the phase signal to obtain enhanced phase measurement accuracy for experiments limited by low photon numbers.

When two complex fields R (reference field) and O (object field) interfere, the interference signal I detected by a square-law detector is represented by

$$I = |R|^2 + |O|^2 + R^*O + RO^*. \tag{1}$$

Given the prior knowledge about R, the typical methods for the analysis of the interference data are linear in nature. The first step in estimating the phase from the interference data is to get rid of the two intensity terms $|R|^2$ and $|O|^2$ in Eq. (1), followed by processing of the remaining cross terms to estimate the amplitude and the phase of the unknown complex field O. The removal of $|R|^2$ and $|O|^2$ may be performed by high-pass filtering of the interference signal I or by using multiple recordings of the interference signal with known phase shifts in R. When the phase of O is smaller than $\pi/2$ in magnitude, a balanced detection scheme such as homodyning [3] may be followed. However, if the phase of O can take any value in the interval $[-\pi,\pi]$, typically four interference signals are recorded with reference phase shifts of $\theta = 0$, $\pi/2$, π, and $3\pi/2$ applied to R [4]. The corresponding four interference records are sufficient to provide information about the two quadratures of the unknown object field O. Denoting the four interference records as I_θ, the phase ϕ_O of the object field relative to the phase ϕ_R of the reference field may be expressed as

$$\phi_O - \phi_R = \arctan\left(\frac{I_{3\pi/2} - I_{\pi/2}}{I_0 - I_\pi}\right). \tag{2}$$

Henceforth, we will refer to this procedure as the phase-shifting method (PSM). Improving the accuracy of the phase estimation is of great interest to all the associated applications, and this problem has been studied in detail in literature [5–8]. It is now well established that when classical-light sources are used, the phase-detection accuracy is ultimately limited by the shot noise or the $\sqrt{N}$ noise, where N is the mean number of photon counts registered by a point detector. This noise limit is often referred to as the SNL. Obtaining phase-detection accuracy below the SNL requires the use of nonclassical states of light such as squeezed or entangled states [9–12]. The introduction of a squeezed vacuum for sub-shot-noise

*kedark@physics.iitd.ac.in

phase detection is now implemented in gravitational wave detection experiments [13,14]. Squeezing enhanced optical phase tracking for optical communication applications has also been demonstrated [15]. Another class of measurements using an adaptive feedback mechanism has been suggested for achieving accuracy below the SNL [16–18]. In the context of optimally estimating a classical Markov process that is coupled to a quantum sensing system, a time-symmetric quantum smoothing framework has been developed and demonstrated experimentally [19,20]. Fundamental quantum limits to time-varying wave-form detection have been discussed recently in the context of a force estimation problem [21,22]. A stochastic Heisenberg limit has also been studied in the context of optimally estimating the time-varying fluctuating phase [23]. In the present work we use a Mach-Zehnder interferometer setup without any additional hardware and illustrate enhanced phase-detection accuracy based on the redundancy or sparsity of the phase function to be measured.

The analysis of interference records that leads to SNL is traditionally performed with point detectors and a phase extraction procedure such as balanced homodyning or phase shifting is assumed. This leads to all the data points in a time domain (e.g., photon counts recorded by a point detector as a function of time) or in a space domain (e.g., pixels of an array detector) being processed in parallel. In most practical applications the underlying solution ϕ_O that one is seeking has some structure (as opposed to random or white noise) and hence the individual measurement points in the interference data may not be treated as independent of each other. Recent developments in the area of compressive sensing [24] suggest that such redundancy in the desired solution may be exploited to achieve excellent signal or image recovery even with data that are traditionally considered incomplete. This expected redundancy in the signal to be recovered is not considered in methods such as PSM, but can be modeled in an optimization framework to gain noise advantage, as we illustrate here.

For the phase measurement problem we consider a constrained optimization formulation [25] where we minimize a cost function of the form [26]

$$C(O,O^*) = ||\beta(I)[I - (|R|^2 + |O|^2 + R^*O + RO^*)]||^2 + \alpha\psi(O,O^*). \quad (3)$$

The first term in the above equation is a weighted L_2-norm squared data fit and the second term is a constraint that models some physically desirable property of the solution O. The choice of $\psi(O,O^*)$ depends on the problem at hand, as we shall explain later. The weights $\beta(I)$ in the first term may be selected such that the measurements with larger photon counts gain more importance in the cost function. The parameter α controls the relative importance of the two terms in the cost function. The knowledge of R is required for both the phase-shifting and the constrained optimization methods in order to determine the amplitude and phase of O. Recently we have demonstrated the advantage of such an approach for achieving single-shot high-resolution digital holographic imaging [26,27]. These experiments were, however, performed at high light level and the issues such as accuracy relative to SNL were of no concern there, as is the case in the present study with low photon level interference data. In order to test the noise characteristics of this optimization approach to phase detection, we performed a low light level interference experiment where a tilted plane wave front and a quadratic wave front were interfered. In order to obtain data that are photon noise limited, we employed a sensitive electron multiplier CCD (EMCCD) array sensor (Andor iXon3) in a photon counting mode. A 128×128 pixel region of the EMCCD was used for all the illustrations below. The schematic setup of our experiment as shown in Fig. 1 consists of a Mach-Zehnder interferometer. The illumination source is a linearly polarized He-Ne laser which is collimated and split at the first beam splitter. The mirror M1 in the reference arm is used to produce a tilt in the plane reference wave front. The lens L ($f = 10$ cm) in the object arm produces an approximately quadratic phase front. The QHQ (Q = quarter-wave plate, H = half-wave plate) arrangement in the reference arm was used as a geometric phase shifter [28] for generating four frames of the phase-shifting interference data. The optimization procedure as in Eq. (3) requires a single interference data frame. A separate interference data frame with the number of photon counts approximately equal to the sum of photon counts in the four phase-shifting frames was thus recorded. This single interference frame was then used with the optimization algorithm. The performance of the phase estimation methods is compared against the average number N_0 of photon counts registered per EMCCD pixel. The total photon resources used for the phase map measurement are thus equal to N_0 times the number of pixels, and this number is equal in both PSM and the optimization method. In our experiments N_0 varied from approximately 800 to 10. Light level reduction was achieved with the help of neutral density filters and by controlling the exposure time (electronic shutter) of the EMCCD array. In order to find a ground truth phase map of the object beam O for a later comparison with the low light level phase reconstructions, a phase-shifting data set with a sufficiently high light level ($N_0 > 5000$) was recorded. This high light level data set is able to give a smooth phase map ϕ_{HLL} for the object beam as shown in Fig. 1(a). In order to

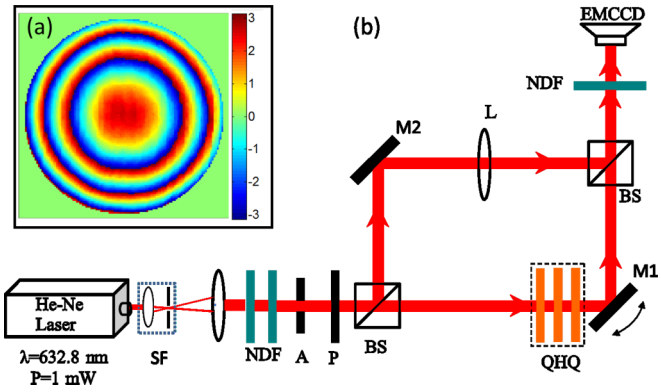

FIG. 1. (Color online) (a) Reference phase map at the sensor plane obtained using high light level (>5000 counts/pixel) phase-shifting data. (b) Experimental setup for the low light level interference experiment. SF: spatial filter; P: polarizer; A: aperture; NDF: neutral density filter; QHQ: geometric phase shifter; L: lens ($f = 10$ cm); BS: beam splitter; M1, M2: mirrors; EMCCD: electron multiplier CCD sensor.

find R, a separate calibration interference pattern was recorded without any object in the object arm of the interferometer, and the straight line fringes were used to estimate the tilt in the reference beam. The constrained optimization procedure was implemented using a gradient descent iteration. Since the cost function is a function of both O and O^*, the steepest descent direction is computed with respect to O^* [29]. The gradient of the cost function in Eq. (3) is given by

$$\nabla_{O^*} C(O,O^*) = -\beta(I)[I-(|R|^2+|O|^2+R^*O+RO^*)](O+R) + \alpha\nabla_{O^*}\psi(O,O^*). \quad (4)$$

The iterative algorithm is then designed such that an updated solution $O^{(n+1)}$ is obtained from the previous solution $O^{(n)}$ as

$$O^{(n+1)} = O^{(n)} - t[\nabla_{O^*} C(O,O^*)]_{O=O^{(n)}}. \quad (5)$$

The step size t may be selected in each iteration by a standard backtracking line search [30]. We used the weights $\beta(I)$ with I in photon count units proportional to $\sqrt{I}$ so that the terms with higher photon counts were weighted by their relative detection signal-to-noise ratio. Further, since the object wave front has resulted due to Fresnel diffraction from the (lens) object, the resultant field O is expected to have a certain degree of smoothness. The smoothness property for the Fresnel diffraction field is expected irrespective of any sharp features that the object may have. This desirable property can be modeled with the penalty term $\psi(O,O^*)$ defined as

$$\psi(O,O^*) = \sum_p \sum_{q\in N_p} w_{pq}|O_p - O_q|^2. \quad (6)$$

The first summation above is over all pixels p in the image, and the pixels q belong to some neighborhood N_p of a particular pixel p. The window function w_{pq} is a decreasing function (e.g., a Gaussian) of the distance between the pixels indexed by p and q. From the nature of $\psi(O,O^*)$ it may be noted that large differences in the numerical value of O at any pixel with those in its neighborhood are penalized and a locally smooth solution as guided by window function w_{pq} is obtained. In practice, we implemented the optimization algorithm by alternatingly minimizing the two terms of the cost function in an adaptive manner in a fashion similar to some recent work in image recovery literature [31,32].

For our experimental data, approximately 15–20 iterations were required in each case to achieve the convergence. The relative change in the solutions from successive iterations was seen to be less than 10^{-3} (or 0.1%) at this stage. Some of the phase recovery results are shown in Figs. 2(a)–2(c). The phase maps for the object field as obtained using the PSM [Eq. (2)] and the corresponding result using the constrained optimization method are shown such that both methods use the same average number of photons per pixel. We clearly observe the advantage of using the constrained optimization procedure by visual comparison of the resultant phase maps with the phase map ϕ_{HLL} as in Fig. 1(a). Denoting the phase maps obtained using the PSM and the constrained optimization approaches as ϕ_{PS} and ϕ_{CO}, respectively, we define the noise

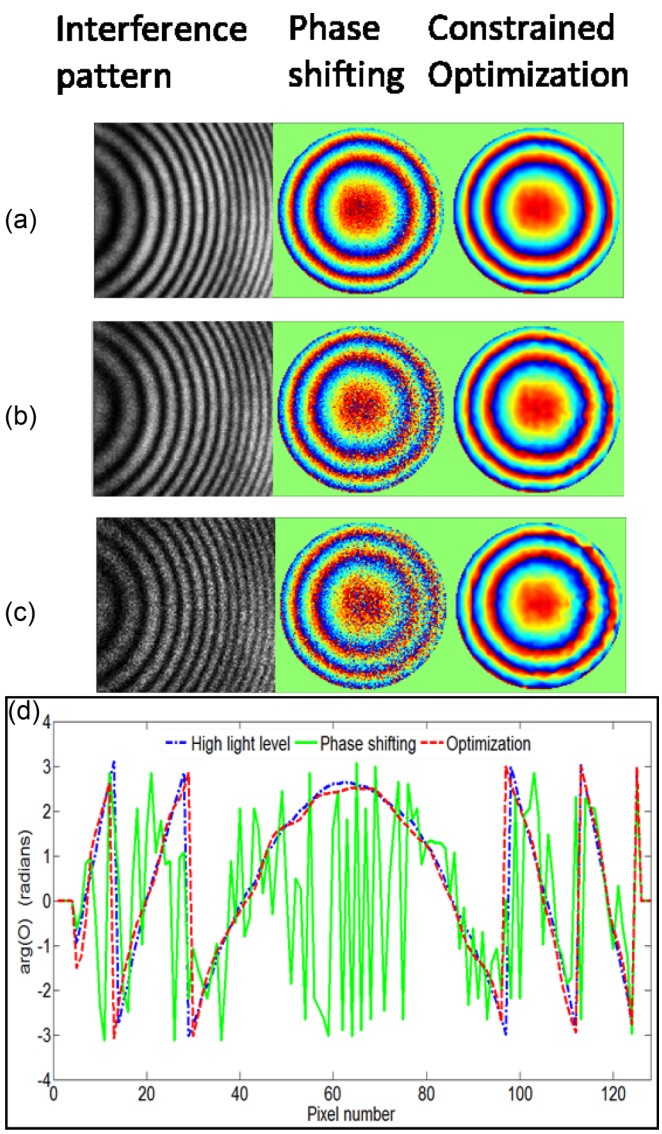

FIG. 2. (Color online) (a)–(c) Single-shot interference patterns used in the optimization method (left column), phase recovery using the PSM (middle column), and the optimization method (right column). The N_0 values in (a)–(c) are 225, 58, and 10, respectively. (d) Phase profiles of the center pixel column of the image ϕ_{HLL} [Fig. 1(a)] and the phase recoveries using PSM and optimization methods as in (c) above for $N_0 = 10$ counts/pixel.

gain as

$$G = \frac{E_{PS}}{E_{CO}} = \frac{||\phi_{HLL} - \phi_{PS}||}{||\phi_{HLL} - \phi_{CO}||}. \quad (7)$$

The gain G is a ratio of the rms (or L_2-norm) phase errors in ϕ_{PS} and ϕ_{CO} with respect to ϕ_{HLL} [Fig. 1(a)]. In Fig. 3, we show log-log plots of the gain G, and the two rms errors E_{PS}, E_{CO} as in Eq. (7) with respect to N_0. E_{PS} is observed to scale as $N_0^{-0.53\pm0.04}$, which is close to the expected shot-noise behavior, whereas E_{CO} is seen to scale as $N_0^{-0.20\pm0.06}$. The noise gain G is seen to scale as $N_0^{-0.33\pm0.04}$. Here the $\pm$ ranges in the scaling relations show a 95% confidence interval for the scaling coefficient for fitting of our data. While we have

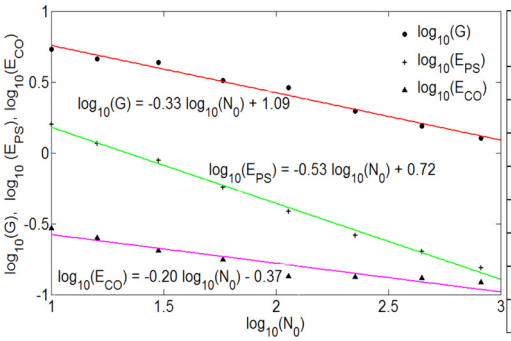

Counts/Pixel (N_0)	Gain (G)
10	5.38
16	4.62
30	4.33
58	3.23
114	2.87
225	1.97
447	1.55
820	1.27

FIG. 3. (Color online) Plot of noise gain G, E_{PS}, and E_{CO} [Eq. (7)] with respect to the average number N_0 of photon counts per pixel (on a log-log scale) used for phase map estimation.

made experimental measurements for N_0 as low as 10 based on detector limitations, our tests on simulated interference patterns for lower photon counts (up to $N_0 = 1$) show that the trend in scaling of E_{PS}, E_{CO}, and G as above continues to hold. An rms error scaling of $N_0^{-0.25}$ has been obtained in a feedback-based interferometric scheme in Ref. [17] for time-varying phase signals. The scaling law obtained by us is, however, likely to change depending on the sparsity in the phase function to be measured. The most important point to note from Fig. 3 is that in the range of N_0 considered, the error E_{CO} for the optimization method is always lower than the error E_{PS} for the phase-shifting method which defines the SNL. Since the two solutions ϕ_{PS} and ϕ_{CO} are almost equal at high light levels, the optimization solution is significantly better as N_0 is reduced, and in this sense the optimization method provides sub-shot-noise performance. For example, if N_0 is reduced by a factor of 2, the PSM solution gets worse by $\approx\sqrt{2}$ whereas the optimization solution gets worse by a factor $2^{0.20} = 1.15$. The weak dependence of E_{CO} on N_0 in the low N_0 range highlights the importance of the smoothness penalty term in the optimization solution. A further analysis leading to a generalized multipixel SNL is required that incorporates the statistics of the light source as well as a measure of redundancy in the phase function ϕ_O that is to be estimated.

The noise gain G may be interpreted in two different ways—when traditional approaches such as PSM are used and ideal detectors are assumed, achieving a similar accuracy as offered by the optimization method will require (i) classical light that is more intense by a factor of G^2 or (ii) nonclassical sub-Poissonian light with fluctuations below the shot noise by a factor of G. In our opinion, the noise gains >5 as observed in our experiments can be significant for sensitive phase-detection applications that are currently considered limited by shot noise. The optimization framework we have used here exploits the redundancy in the function ϕ_O to achieve improved phase-detection accuracy even when a classical-light source is used. We expect further improvement in phase-detection accuracy if nonclassical states of light (e.g., squeezed states, spatially entangled light fields) or schemes such as adaptive feedback [16,17] are used in combination with this optimization-based approach to phase estimation. While we have considered a stationary two-dimensional (2D) wave front in this work, a similar approach will apply equally well if a series of interference data points is recorded in time with a point detector and an appropriate penalty term is designed that models the desirable properties of a time-varying phase function. Also, we are not restricted to the smoothness penalty function as used in this work—other forms of penalties such as L_1-norm based penalties (e.g., total variation) or generalized Gibbs priors [33] may well be used if required.

In conclusion, our work suggests that noise performance better than conventional single-pixel-based SNL for phase detection in an interference experiment may be achievable even with classical light if an optimization approach to phase detection as described here is used. Any interferometric scheme (using either classical or nonclassical states of light) is expected to benefit from such an approach to achieve enhanced phase-detection sensitivity. The limits such as SNL that are traditionally defined with considerations of the statistics of the light source alone may thus be generalized to take into account the redundancy in the phase signal that we intend to measure.

The authors acknowledge discussions with Dr. V. Ravishankar and Dr. M. S. Santhanam. M.S. and K.K. acknowledge support from Department of Biotechnology, Ministry of Science and Technology, India Grant No. BT/PR8008.

[1] P. Hariharan, *Basics of Interferometry* (Academic, New York, 2007).
[2] B. P. Abbott *et al.*, Rep. Prog. Phys. **72**, 076901 (2009).
[3] H. Haus, *Electromagnetic Noise and Quantum Optical Measurements* (Springer, Berlin, 2000).
[4] I. Yamaguchi and T. Zhang, Opt. Lett. **22**, 1268 (1997).
[5] J. F. Walkup and J. W. Goodman, J. Opt. Soc. Am. **63**, 399 (1973).
[6] C. M. Caves, Phys. Rev. D **23**, 1693 (1981).
[7] M. T. Jaekel and S. Reynaud, Europhys. Lett. **13**, 301 (1990).
[8] F. Charrier, B. Rappaz, J. Kuhn, T. Colomb, P. Marquet, and C. Depeursinge, Opt. Express **15**, 8818 (2007).
[9] M. Xiao, L. A. Wu, and H. J. Kimble, Phys. Rev. Lett. **59**, 278 (1987).
[10] P. Grangier, R. E. Slusher, B. Yurke, and A. La Porta, Phys. Rev. Lett. **59**, 2153 (1987).
[11] B. Yurke, Phys. Rev. Lett. **56**, 1515 (1986).
[12] M. O. Scully and J. P. Dowling, Phys. Rev. A **48**, 3186 (1993).
[13] R. Schnabel, N. Mavalvala, D. E. McClelland, and P. K. Lam, Nat. Commun. **1**, 121 (2010).
[14] H. Grote, K. Danzmann, K. L. Dooley, R. Schnabel, J. Slutsky, and H. Vahlbruch, Phys. Rev. Lett. **110**, 181101 (2013).
[15] H. Yonezawa, D. Nakane, T. A. Wheatley, K. Iwasawa, S. Takeda, H. Arao, K. Ohki, K. Tsumura, D. W. Berry, T. C. Ralph, H. M. Wiseman, E. H. Huntington, and A. Furusawa, Science **337**, 1514 (2012).
[16] H. M. Wiseman and R. B. Killip, Phys. Rev. A **56**, 944 (1997).

[17] D. W. Berry and H. M. Wiseman, Phys. Rev. A **65**, 043803 (2002).
[18] D. W. Berry and H. M. Wiseman, Phys. Rev. A **73**, 063824 (2006).
[19] M. Tsang, Phys. Rev. Lett. **102**, 250403 (2009).
[20] T. A. Wheatley, D. W. Berry, H. Yonezawa, D. Nakane, H. Arao, D. T. Pope, T. C. Ralph, H. M. Wiseman, A. Furusawa, and E. H. Huntington, Phys. Rev. Lett. **104**, 093601 (2010).
[21] M. Tsang, H. M. Wiseman, and C. M. Caves, Phys. Rev. Lett. **106**, 090401 (2011).
[22] M. Tsang and R. Nair, Phys. Rev. A **86**, 042115 (2012).
[23] D. W. Berry, M. J. W. Hall, and H. M. Wiseman, Phys. Rev. Lett. **111**, 113601 (2013).
[24] E. Candes, J. Romberg, and T. Tao, IEEE Trans. Inf. Theory **52**, 489 (2006).
[25] M. Bertero and P. Boccacchi, *Introduction to Inverse Problems in Imaging* (IOP, London, 1998).
[26] K. Khare, P. T. Samsheerali, and J. Joseph, Opt. Express **21**, 2581 (2013).
[27] P. T. Samsheerali, K. Khare, and J. Joseph, Opt. Commun. **319**, 85 (2014).
[28] N. Mukunda and R. Simon, Ann. Phys. **228**, 205 (1993).
[29] D. H. Brandwood, Proc. IRE **130**, 11 (1983).
[30] S. Boyd and L. Vandenberghe, *Convex Optimization* (Cambridge University Press, Cambridge, UK, 2004).
[31] E. Y. Sidky and X. Pan, Phys. Med. Biol. **53**, 4777 (2008).
[32] L. Ritschl, F. Bergner, C. Fleischmann, and M. Kachelriess, Phys. Med. Biol. **56**, 1545 (2011).
[33] S. Geman and D. Geman, IEEE Trans. Pattern Anal. Mach. Intell. **PAMI-6**, 721 (1984).